Interaction of Lamb Waves with Fatigue Cracks in Aluminum

E. D. SWENSON, C. T. OWENS and C. ALLEN

ABSTRACT

Elastic waves can travel across relatively large distances in thin metallic plates, and can be affected by discontinuities such as cracks. This paper presents an investigation of the interaction of Lamb waves with both open and closed low-cycle fatigue cracks in aluminum plates using a three-dimensional laser Doppler vibrometer (3D-LDV). The 3D-LDV provides measurements of both in- and out-of-plane velocity components over a uniform grid of up to ~27,000 points with approximately 0.7 mm spacing in the x- and y-directions. Images created from the 3D-LDV measurements clearly show the interaction of the elastic wave energy with the cracks. Comparisons between in- and out-of-plane components provide insight into whether and how the propagation behaviors of symmetric and antisymmetric Lamb wave modes differ upon encountering fatigue cracks.

INTRODUCTION

The use of guided elastic waves (Lamb waves) has shown promise in detecting highly localized damage, such as cracking, due to the relatively short wavelength of the propagating waves. As such, Lamb waves offer multiple advantages for structural health monitoring (SHM) applications, such as the ability to propagate over relatively large distances (improving the ability to monitor large areas for relatively small damage) and to providing through-thickness interrogation (which may be of particular importance in detecting internal defects). Staszewski, *et al.* [1-4] demonstrated the potential of laser vibrometry as a large-area measurement and detection tool for fatigue cracking in metallic plates. While the size and cost of current LDVs limit their use in practical SHM applications, insight gained in laboratory experiments will hopefully lead to improvements in elastic wave modeling and simulation. Such improvement is vital to the design and implementation of practical and robust online SHM systems for aerospace structures in the future.

This paper presents initial studies on three aluminum plate test specimens with

---

The views expressed in this paper are those of the authors and do not reflect the official policy or position of the US Air Force, Department of Defense, or US Government.

Eric D. Swenson, Air Force Institute of Technology, AFIT/ENY, Wright-Patterson AFB, Dayton, OH, 45433, USA

Report Documentation Page

Form Approved
OMB No. 0704-0188

1. REPORT DATE	2. REPORT TYPE	3. DATES COVERED
SEP 2011	**N/A**	**-**

4. TITLE AND SUBTITLE	5a. CONTRACT NUMBER
Interaction of Lamb Waves with Fatigue Cracks in Aluminum	5b. GRANT NUMBER
	5c. PROGRAM ELEMENT NUMBER
6. AUTHOR(S)	5d. PROJECT NUMBER
	5e. TASK NUMBER
	5f. WORK UNIT NUMBER
7. PERFORMING ORGANIZATION NAME(S) AND ADDRESS(ES) **Air Force Institute of Technology, AFIT/ENY, Wright-Patterson AFB, Dayton, OH, 45433, USA**	8. PERFORMING ORGANIZATION REPORT NUMBER
9. SPONSORING/MONITORING AGENCY NAME(S) AND ADDRESS(ES)	10. SPONSOR/MONITOR'S ACRONYM(S)
	11. SPONSOR/MONITOR'S REPORT NUMBER(S)

12. DISTRIBUTION/AVAILABILITY STATEMENT
Approved for public release, distribution unlimited

13. SUPPLEMENTARY NOTES
See also ADA580921. International Workshop on Structural Health Monitoring: From Condition-based Maintenance to Autonomous Structures. Held in Stanford, California on September 13-15, 2011 . U.S. Government or Federal Purpose Rights License.

14. ABSTRACT
Elastic waves can travel across relatively large distances in thin metallic plates, and can be affected by discontinuities such as cracks. This paper presents an investigation of the interaction of Lamb waves with both open and closed low-cycle fatigue cracks in aluminum plates using a three-dimensional laser Doppler vibrometer (3D-LDV). The 3D-LDV provides measurements of both in- and out-of-plane velocity components over a uniform grid of up to ~27,000 points with approximately 0.7 mm spacing in the x- and y-directions. Images created from the 3D-LDV measurements clearly show the interaction of the elastic wave energy with the cracks. Comparisons between in- and out-of-plane components provide insight into whether and how the propagation behaviors of symmetric and antisymmetric Lamb wave modes differ upon encountering fatigue cracks.

15. SUBJECT TERMS

16. SECURITY CLASSIFICATION OF:			17. LIMITATION OF ABSTRACT	18. NUMBER OF PAGES	19a. NAME OF RESPONSIBLE PERSON
a. REPORT	b. ABSTRACT	c. THIS PAGE			
unclassified	**unclassified**	**unclassified**	**SAR**	**8**	

fatigue cracks of various lengths. Details on the experimental setup and and LDV testing are provided. Finally, experimental results are presented and discussed, followed by conclusions and recommendations.

EXPERIMENTAL TESTING

Test Article Preparation

The test specimens were 3.175 mm (0.125 in) thick 6061-T6 aluminum plates cut into a "dogbone" shape (Fig. 1(a)). Overall dimensions were 610 mm x 305 mm (24 in x 12 in), with a test section of 305 mm x 254 mm (12 in x 10 in). A 1.59 mm (0.0625 in) hole was drilled in the center of each specimen in order to facilitate fatigue crack growth. Each specimen was mounted in a set of mild steel grips using 12.7 mm (0.5 in) diameter grade 8 bolts and loaded in a 500 kN (110 kip) Material Test Systems uniaxial fatigue test machine (Fig. 1(b)).

The plates were each subjected to sinusoidal cyclic loading at 8 Hz with nominal maximum and minimum load values of 173 kN (39 kip) and 17.3 kN (3.9 kip), respectively. The first specimen was subject to variation in max/min load during the initial tuning of the fatigue test machine and the total number of cycles was not accurately recorded. After an estimated 30,000 cycles, a ~53 mm crack

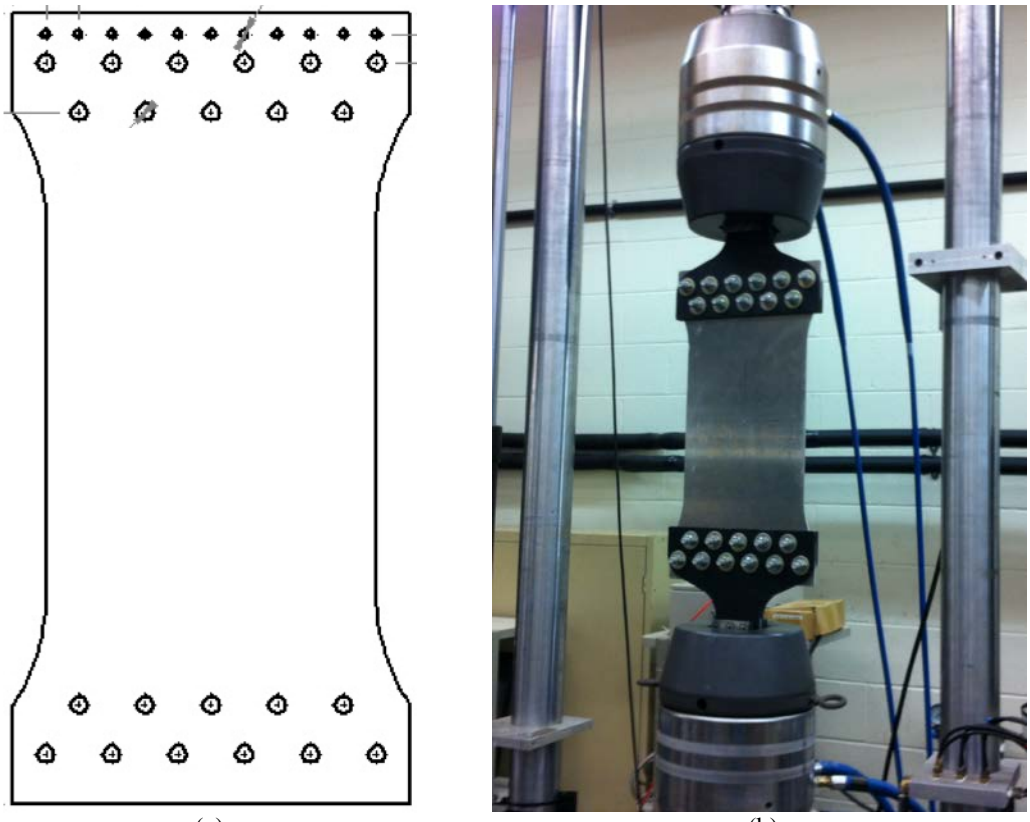

(a) (b)

Figure 1: (a) Profile view of "dogbone" specimen, (b) Test specimen in MTS fatigue test machine

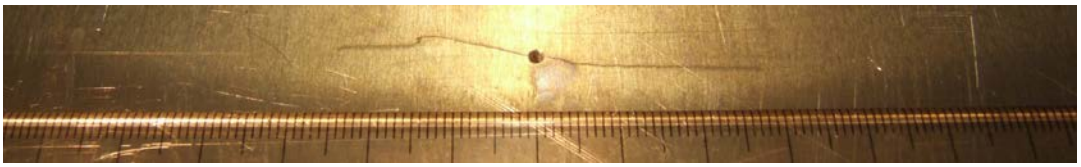

(a) C53L

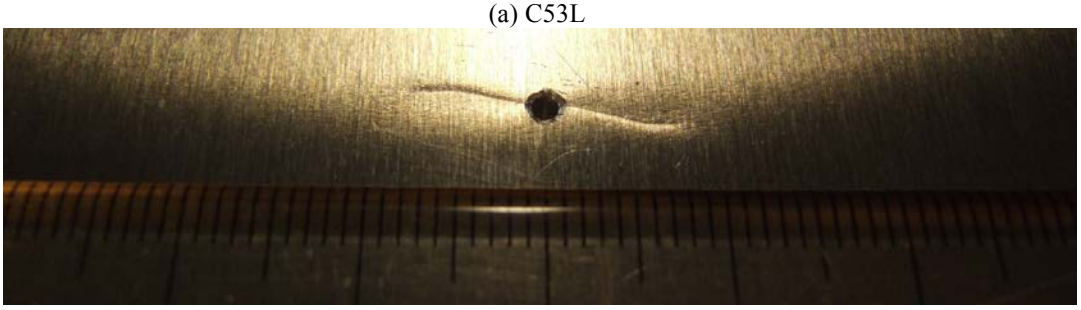

(b) C15L

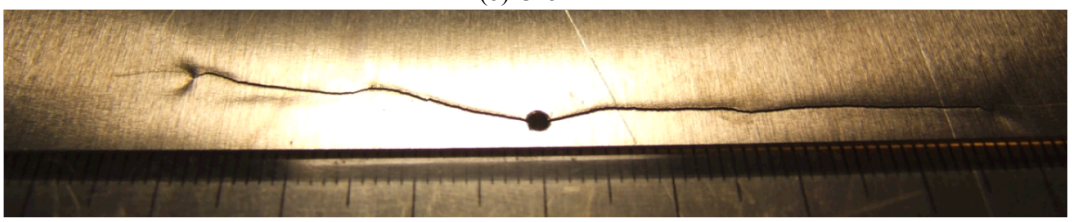

(c) C85L

Figure 2: (a) 53 mm Closed Crack, (b) 15 mm Closed Crack, (c) 85 mm Open/Closed Crack

had grown from the center hole (Fig. 2(a)) and load cycling was terminated. Load cycling of the second specimen was halted after 21,000 cycles, at which point a ~15 mm crack had been established (Fig. 2(b)). The final specimen underwent 26,000 cycles at the loads listed above, which produced a ~31 mm crack. The max/min load was reduced to 133/13.3 kN (30/3.0 kip) and another 8,000 cycles were applied to produce a total crack length of ~67 mm. At this point a 173 kN (39 kip) static load was applied, resulting in significant plastic deformation at the crack tips and a permanently "open" crack. The max/min load was reduced again to 120/12.0 kN (27/2.7 kip) and 2,000 additional cycles applied. This produced a short closed crack emanating from either end of the open crack and a total crack length of ~85 mm (Figure 2c). The three specimens were designated C53L, C15L, and C85L (C - center hole, ## - approximate crack length in mm, L - low-cycle fatigue). In addition, an uncracked plate with an identical center hole, designate C0 was included as a baseline.

A single 6.35 mm diameter x 0.254 mm thick PZT transducer was bonded approximately on the longitudinal centerline of plates C0, C15L, and C53L at distances of 30, 40, and 50 mm, respectively, from the hole (center of hole to center of PZT) using M-Bond 200 adhesive. An identical PZT was bonded approximately 40 mm from the hole, but 25 mm offset from the longitudinal centerline of C85L. These transducers were used to induce Lamb waves in the plates.

For the experimental testing, a Hamming-windowed, 5-1/2 cycle sine burst excitation signal was generated using an Agilent 33120A arbitrary waveform generator. This signal was amplified using a Krone-Hite 7500 wideband power amplifier to between 100 and 200 Vpp and applied to the PZT transducers. In prior experiments [5], pitch-catch testing was performed on a similar 3 mm aluminum

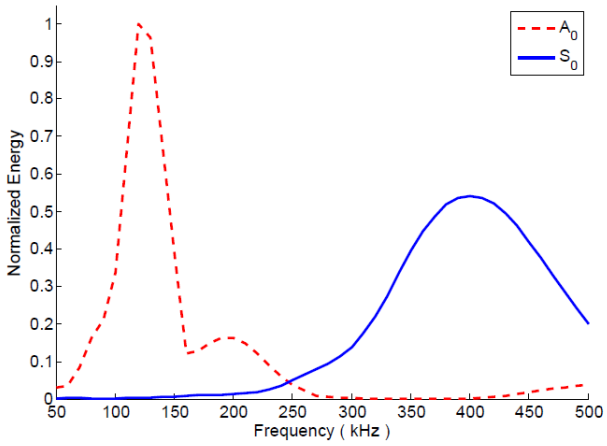

Figure 3: Normalized Wave Energy vs Frequency for A_0 and S_0 Modes in 3 mm Aluminum Plate

plate and the data used to create Lamb wave mode tuning curves. These curves identify appropriate frequencies to excite primarily A_0 or S_0, or both modes equally (Figure 3). Excitation at a center frequency of 100 kHz dominantly excites the A_0 mode, amplitudes of A_0 and S_0 are approximately equal at 250 kHz, and at 300 kHz and above, S_0 is the dominant mode.

Data collection ws performed using a Polytec PSV-400-3D-M scanning laser Doppler vibrometer system designed for full-field vibration measurements at frequencies up to 1MHz. The system consists of a motorized PSV-A-T31 tripod, supporting 3 separate PSV-I-400 sensor heads, as well as a high-resolution camera that provides the capability to make precise corrections to the measurement scan points in 3D. Surface velocity measurements are made by evaluating the Doppler frequency shift of a laser beam reflected from the test article. Each sensor head can only measure velocity along the axis of its laser beam. For 3D measurements, the sensor heads are calibrated and all three laser spots are placed at a coincident point on the test article surface. The raw measurements from the three heads, are combined with the beam angle data in the data processing computer in order to resolve the velocity data onto an orthogonal 3D coordinate system. In this manner, the system allows for fast, precise, non-contact 3D surface velocity measurements. In order to maximize return laser energy to each sensor head, retro-reflective film was applied to each of the test articles.

TABLE I: SCAN GRID PARAMETERS (values are approximate)

Test Specimen	X Dimension (mm)	Y Dimension (mm)	No. of Scan Points
C0	43	43	4,000
C15L	60	77	9,200
C53L	141	96	27,300
C85L	154	76	23,800

All test articles were scanned using a rectangular grid at approximately 0.7 mm spacing in the x- and y-directions, centered on the hole. The scan area dimensions and point counts were as described in TABLE I. In all cases, the x- and y-axes are defined as being in the plane of the plate, and the z-axis is out-of-plane. All measurements were based on 30 averages and a band pass filter with cutoff frequencies ±50 kHz from the excitation center frequency was applied to each sample as it was collected. Measurements were performed at a sample rate of 2.56 MHz for 512 samples, resulting in ~200 μsec of data at each sample point. Data was collected at excitation center frequencies of 100, 200, 250, and 300 kHz; however, only 250 kHz data is presented in the paper due to space limitations.

RESULTS

Figure 4 shows both the in-plane and out-of-plane RMS velocity plots at the 250 kHz excitation center frequency for all three crack configurations as well as the uncracked plate. Waves are propagated from top to bottom and cracks are depicted as solid black lines. The small white areas in the center represent scan points that lay either in or too near the center hole and were therefore disabled. Velocity scaling was adjusted separately for each each image in order to best highlight features of interest.

In the cases of all three cracked specimens, constructive interference from reflected wave energy creates increased RMS intensity along the top edge (towards the PZT) of the cracks as compared to the RMS plots of C0. This effect is present for both the in-plane and out-of plane plots, though it appears to be stronger for the in-plane cases. The shape and overall size of the two longer cracks are well outlined by these regions of higher RMS velocity. Additionally, the plots show a significant decrease in velocity on the lee side of the cracks (opposite the PZT) as compared to the uncracked specimen, indicating less wave energy is reaching these areas due to the reflection and diffraction effects of the cracks. The plots of C85L,

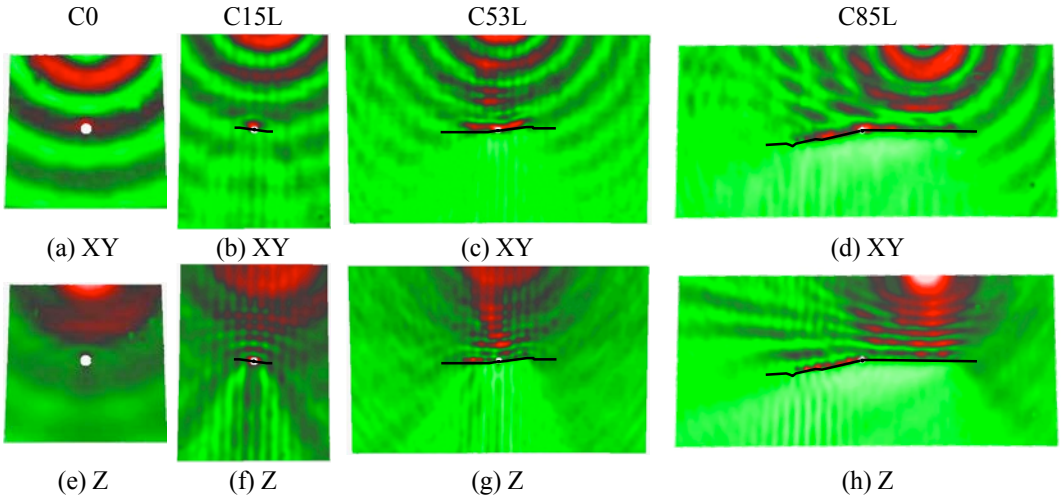

Figure 4: RMS velocity @ 250 kHz excitation frequency: (a – d) in-plane, (e – h) out-of-plane

in particular, show an area of almost zero velocity on the lee side of the crack (seen as a very lightly shaded region). This is due to the majority of the crack being open—no discernable wave energy is transmitted directly across the crack.

Figures 5 thru 7 show both in-plane and out-of-plane wave velocity fields at three separate time steps for each of the three cracked specimens. The first snapshot is after the leading edge of the S_0 wave packet has passed, but before the A_0 packet has reached the crack. The second time step is during the A_0 packet's transition of the crack. The final time step is just after the majority of the A_0 packet has passed the crack and reflection/interference patterns are clearly visible.

Densely spaced 3D-LDV measurements make it possible to visualize how wave energy behaves (reflection/diffraction/mode-conversion) as it transitions the crack region. While separate in-plane and out-of-plane data help, they do not provide completely isolated measurements of symmetric and anti-symmetric modes. Due to its higher speed, the longer wavelength S_0 energy can clearly be seen in both the in- and out-of-plane measurements at the first time step. However, as the A_0 wave packet arrives, it becomes difficult to distinguish the reflecting S_0 waves, even when focusing on the in-plane plots. By the last time step, the majority of S_0 energy has traveled outside the scan region and both the in- and out-of-plane plots are dominated by A_0.

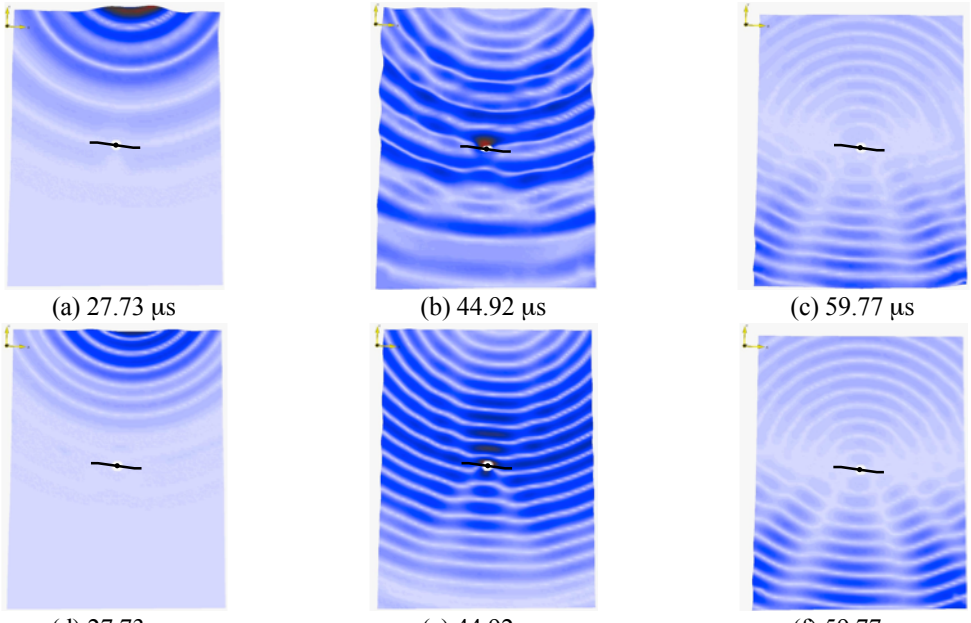

(a) 27.73 μs (b) 44.92 μs (c) 59.77 μs

(d) 27.73 μs (e) 44.92 μs (f) 59.77 μs

Figure 5: C15L velocity at various times: (a – c) in-plane, (d – f) out-of-plane

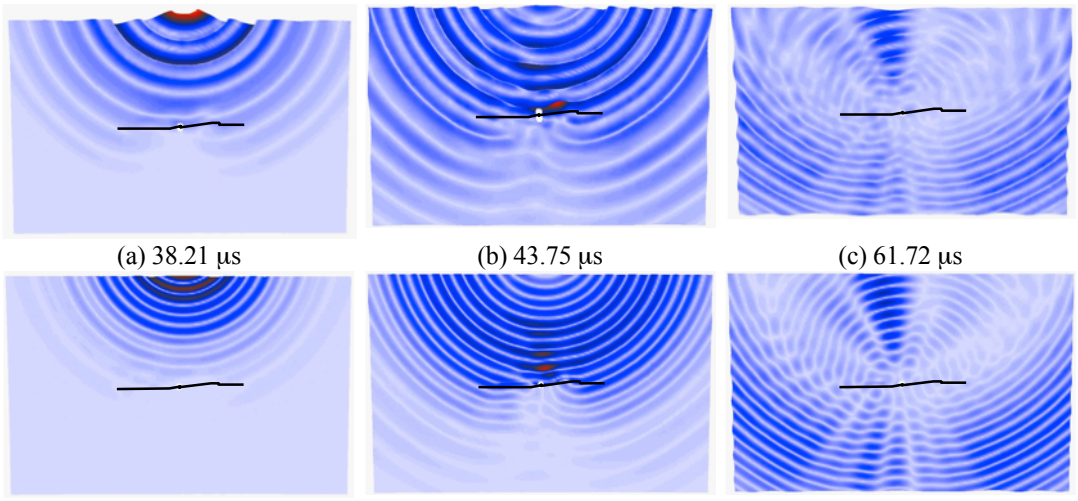

(a) 38.21 μs (b) 43.75 μs (c) 61.72 μs

(d) 38.21 μs (e) 43.75 μs (f) 61.72 μs

Figure 6: C53L velocity at various times: (a – c) in-plane, (d – f) out-of-plane

CONCLUSIONS

This paper demonstrated the successful use of a 3D-LDV for the measurement and visualization of Lamb wave propagation in aluminum plates with varying length cracks. The capabilities of the 3D-LDV allow for fast and accurate measurements of both in-plane and out-of-plane plate velocities. Though not quantified, the presence of 15 and 53 mm closed as well as an 85 mm open crack measurably affected the propagation of Lamb waves as seen in both RMS velocity plots and time-varying wave field velocities.

Planned future work includes measurements of additional fatigue crack samples, comparison of 3D-LDV and UHF-LDV measurements, and detailed numerical analysis to quantify differences in propagation behavior between various types of fatigue damage (high-cycle vs. low-cycle) and undamaged plates.

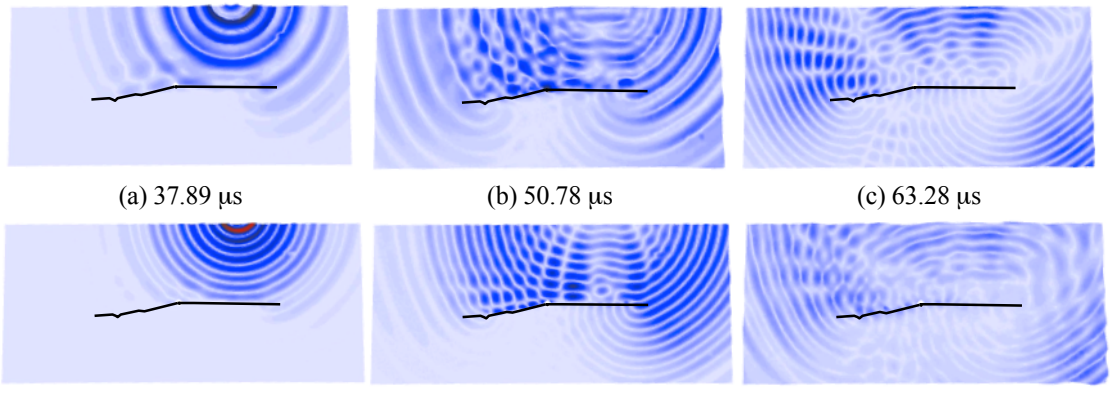

(a) 37.89 μs (b) 50.78 μs (c) 63.28 μs

(d) 37.89 μs (e) 50.78 μs (f) 63.28 μs

Figure 7: C85L velocity at various times: (a – c) in-plane, (d – f) out-of-plane

REFERENCES

1. Staszewski, W.J., Lee, B.C., Mallet, L., and Scarpa, F. 2004. "Structural Health Monitoring using Scanning Laser Vibrometry: I. Lamb Wave Sensing," *Smart Mater. Struct.*, 13: 251-260.
2. Mallet, L., Lee, B.C., Stasqewski, W.J., and Scarpa, F. 2004. "Structural Health Monitoring using Scanning Laser Vibrometry: II. Lamb Waves for Damage Detection," *Smart Mater. Struct.,* 13: 261-269.
3. Leong, W.H., Staszewski, W.J., Lee, B.C., and Scarpa, F. 2005. "Structural Health Monitoring using Scanning Laser Vibrometry: III. Lamb Waves for Fatigue Crack Detection," *Smart Mater. Struct.*, 14: 1387-1395.
4. Staszewski, W.J., Lee, B.C., and Traynor, R. 2007. "Fatigue Crack Detection in Metallic Structures with Lamb Waves and 3D Laser Vibrometry," *Meas. Sci. Technol.*, 18: 727-739.
5. Underwood, R. March 2008. "Damage Detection Analysis using Lamb Waves in Restricted Geometry for Aerospace Applications," Master's Thesis, Air Force Institute of Technology.